IVYSPRING INTERNATIONAL PUBLISHER

Theranostics

2018; 8(12): 3331-3347. doi: 10.7150/thno.25276

Research Paper

Precision-guided long-acting analgesia by Gel-immobilized bupivacaine-loaded microsphere

Wenjing Zhang[1,2], Cong Ning[2,3], Weiguo Xu[2], Hanze Hu[4], Mingqiang Li[4,5,✉], Guoqing Zhao[1,✉], Jianxun Ding[2,✉], Xuesi Chen[2]

1. Department of Anesthesia, China-Japan Union Hospital of Jilin University, Changchun 130033, P. R. China
2. Key Laboratory of Polymer Ecomaterials, Changchun Institute of Applied Chemistry, Chinese Academy of Sciences, Changchun 130022, P. R. China
3. Department of Spine Surgery, The First Hospital of Jilin University, Changchun 130021, P. R. China
4. Department of Biomedical Engineering, Columbia University, New York, NY 10027, United States
5. Guangdong Provincial Key Laboratory of Liver Disease, The Third Affiliated Hospital of Sun Yat-sen University, Guangzhou 510630, P. R. China

✉ Corresponding authors: Jianxun Ding (jxding@ciac.ac.cn), Guoqing Zhao (guoqing@jlu.edu.cn), Mingqiang Li (ml3777@columbia.edu)

Received: 2018.02.01; Accepted: 2018.04.08; Published: 2018.05.23

Abstract

Peripheral nerve blockade (PNB) is a conventional strategy for the management of acute postoperative pain. However, the short duration of the associated analgesia and the potential systemic toxicity due to the low molecular weights of local anesthetics limit their application.

Methods: An *in situ* forming injectable Gel−microsphere (Gel−MS) system consisting of PLGA−PEG−PLGA Gel (Gel) and Gel-immobilized bupivacaine-loaded microsphere (MS/BUP) was prepared for precision-guided long-acting analgesia. A series of *in vitro* characterizations, such as scanning electron microscopy, rheology analysis, confocal laser scanning microscopy, drug release, and erosion and degradation, were carried out. After that, the *in vivo* analgesia effect of the Gel−MS system, the immobilization effect of Gel on the MS, and biocompatibility of the system were evaluated using a sciatic nerve block model.

Results: The BUP release from the Gel−MS system was regulated by both the inner MS and the outer Gel matrix, demonstrating sustained BUP release *in vitro* for several days without an initial burst release. More importantly, incorporation of the Gel immobilized the MS and hindered the diffusion of MS from the injection site because of its *in situ* property, which contributed to a high local drug concentration and prevented systemic side effects. *In vivo*, a single injection of Gel−MS/BUP allowed rats to maintain sensory and motor blockade significantly longer than treatment with MS/BUP ($P < 0.01$) or BUP-loaded Gel (Gel−BUP, $P < 0.01$). Histopathological results demonstrated the excellent biodegradability and biocompatibility of the Gel−MS system without neurotoxicity.

Conclusion: This precision-guided long-acting analgesia, which provides an *in situ* and sustained release of BUP, is a promising strategy for long-acting analgesia, and could represent a potential alternative for clinical pain management.

Key words: injectable Gel, microsphere, *in situ*, bupivacaine, analgesia, medical device

Introduction

Acute postoperative pain is a common and challenging problem, usually occurring within 48 h after surgery [1]. It affects the quality of life, functional recovery, and compliance of patients, resulting in increased postoperative morbidity and delay in hospital discharge. Moreover, acute postoperative pain may become chronic with inadequate pain management [2]. Relief can be obtained by the administration of antipyretic analgesics (*e.g.*, acetaminophen and celecoxib) and

opioids (*e.g.*, morphine and oxycodone). However, these medications, especially opioids, have severe side effects, such as nausea, vomiting, and respiratory inhibition, and may cause tolerance. Recently, the induction of peripheral nerve blockade (PNB) using local anesthetics has attracted considerable attention because of their ability to relieve pain with few complications and low opioid consumption [3]. However, owing to the low molecular weight of anesthetics, the duration of the analgesia induced by a single injection is usually only a few hours, which does not meet the requirements for clinical applications [4]. The conventional approach to achieve prolonged analgesia is the continuous infusion of anesthetics through a catheter. Although this approach does relieve pain, it suffers from some limitations. Firstly, catheter insertion is expensive and technically demanding, requiring the skill of professionals in a hospital. Moreover, it is frequently accompanied by complications, such as catheter abscission, epidural hematoma, and nerve damage [5]. Thus, there is a need for the development of local anesthetic formulations with longer-lasting effects that can be administered as a single injection [6].

A variety of sustained-release formulations, including microspheres [7], microgels [8], Gels [9], nanoparticles [10], liposomes [11], and solid lipid nanoparticles [12], have been investigated to extend the duration of analgesia induced by local anesthetics. Recently, the poly(lactic-*co*-glycolic acid) microspheres (PLGA MSs) have gained in popularity due to their excellent biodegradability, biocompatibility, and stable physicochemical properties during manufacturing and storage [13, 14]. PLGA MSs have been successfully loaded with lidocaine [15], bupivacaine [16], ropivacaine [17], and other local anesthetics, achieving nerve blockade durations of 6−24 h. However, the poor *in situ* properties of MSs and the initial burst release of drugs can reduce blockade duration, and result in local and systemic toxicity [16, 18]. Additionally, MSs tend to fuse physically and clog the needle, hindering their clinical applications [19]. The Gel-MS (Gel−MS) formulation would resolve these problems.

Poly(lactic acid-*co*-glycolic acid)-*block*-poly(ethylene glycol)-*block*-poly(lactic acid-*co*-glycolic acid) (PLGA−PEG−PLGA) triblock polymer has been reported to form thermosensitive Gel (termed as Gel in this study) for drug delivery [20], post-surgical anti-adhesion [21], and tissue engineering applications [22]. At low temperatures (*e.g.*, 4 °C), drugs and cells can be mixed into a polymer solution for convenient injection. As the temperature reaches body temperature, the micelles automatically transform into a viscous gel, forming an *in situ* depot. Thus, the gelation system can achieve sustained drug release *in situ* [23, 24]. The Gel is biodegradable and biocompatible, with easily tuned physicochemical properties during the manufacturing process, making it a safe and controllable drug delivery system. Moreover, the thermosensitive polymer can be injected through an ordinary needle. The use of the thermosensitive Gel reduces the risks of local diffusion, syringe clogging, and the incomplete administration of MSs and nanoparticles [25, 26].

Recently, Gel-MS system that consists of MSs and thermosensitive Gels have attracted extensive attention owing to the following advantages: 1) controllable *in situ* immobilization of the microsphere and avoidance of unexpected particle diffusion; 2) longer half-life and zero-order release kinetics of loaded drugs; 3) excellent biocompatibility without inflammation reaction or formation of granuloma. Generally, Gel-MS systems have been applied for anti-tumor treatment, hypoglycemia, wound healing, and tissue engineering, and has shown great potential in the treatment of a variety of diseases [27-29]. However, only a small number of studies have investigated the application of Gel-MS systems for long-acting analgesia. The few studies that have been conducted so far just focused on the *in vitro* anesthetic release and are lack of *in vivo* evidence for local analgesia [30, 31].

In this context, an injectable Gel-MS system with bupivacaine free base (BUP), denoted as Gel−MS/BUP, was developed to prolong PNB and avoid the associated side effects (**Scheme 1**). In this system, the MS/BUP provides a constant and prolonged release of BUP, while the addition of Gel reduced the initial burst drug release. Moreover, the *in situ* properties of the Gel prevent diffusion of the MSs to distant muscles and ensure high local drug concentration, which is crucial for PNB. The sustained and *in situ* drug release from Gel−MS/BUP is hypothesized to prolong the duration of blockade without toxicity. To have its long-acting analgesic effect and biocompatibility confirmed, the formulation was injected *in vivo* using a rat sciatic nerve block model, sensory and motor blockade was measured, and follow-up histopathological detections were carried out.

Methods

Materials

Bupivacaine hydrochloride (BUP·HCl) was purchased from Beijing Huafeng United Technology Co., Ltd. (Beijing, P. R. China). L-Lactide (L-LA) and glycolide (GA), and PLGA (number-average molecular weight (M_n) = 3.7 kDa) were obtained from

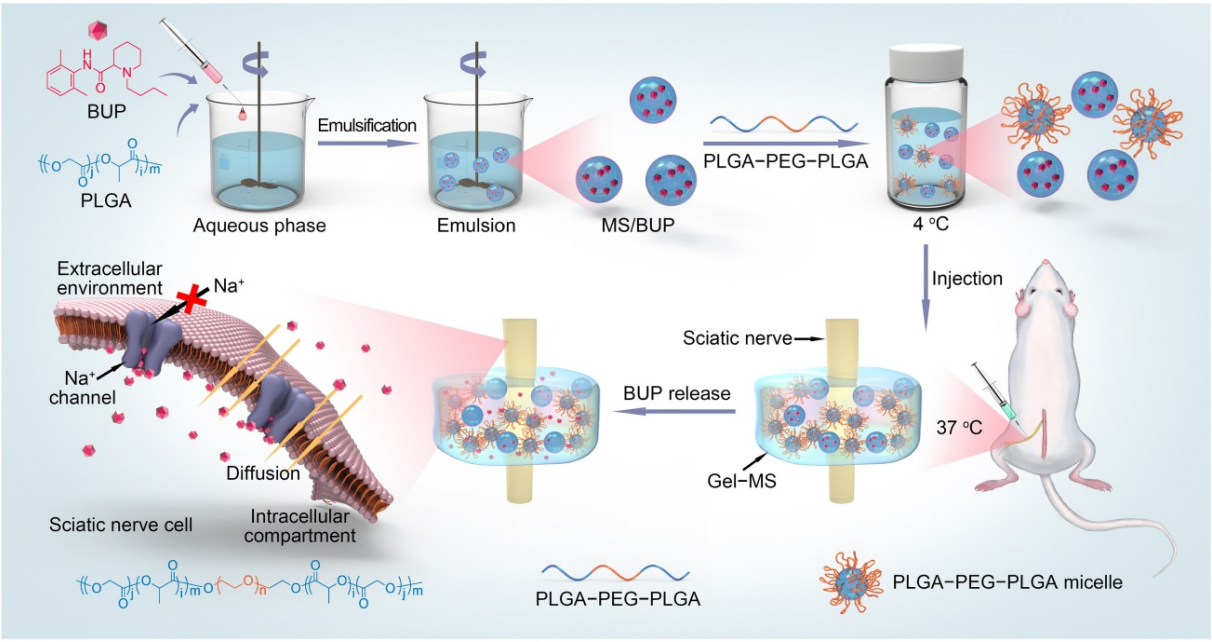

Scheme 1. Schematic illustration of the preparation and *in vivo* nerve blockade effect of the Gel–microsphere system with bupivacaine (Gel–MS/BUP).

Changchun SinoBiomaterials Co., Ltd. (Changchun, P. R. China). PEG (M_n = 1,000 g mol^{-1}) and stannous octoate ($Sn(Oct)_2$) were purchased from Sigma-Aldrich (Shanghai, P. R. China). PLGA–PEG–PLGA (M_n = 4,200 g mol^{-1}, LA/GA = 75:25, mol/mol) was synthesized through the ring-opening polymerization (ROP) of L-LA and GA with PEG as a macroinitiator and $Sn(Oct)_2$ as a catalyst. Poly(vinyl alcohol) (PVA), Nile red (NR), and sodium hydroxide (NaOH) were purchased from Shanghai Chemical Reagent Co., Ltd. (Shanghai, P. R. China). Dichloromethane (DCM), dimethyl formamide (DMF), dimethyl aminopyridine (DMAP), elastase, and 1-(3-dimethylaminopropyl)-3-ethylcarbodiimide hydrochloride (EDC·HCl) were from Aladdin Reagent Co., Ltd. (Shanghai, P. R. China). Coumarin 6 (C6), rhodamine B (RhB), and 4′,6-diamidino-2-phenylindole dihydrochloride (DAPI) were from Sigma-Aldrich (Shanghai, P. R. China).

Preparation of bupivacaine free base

Bupivacaine free base (BUP) was obtained using an alkali deposition method [1]. Briefly, BUP·HCl (5.0 g) was dissolved in 300.0 mL of Milli-Q water, and NaOH (1.0 g) was dissolved in 50.0 mL of Milli-Q water. The NaOH solution was dropwise added into the BUP·HCl solution to induce alkali deposition of BUP. The precipitated base was filtered and repeatedly washed with Milli-Q water until the filtrate was neutral, lyophilized, and stored for further use.

Preparation of drug-loaded microsphere

The BUP-loaded microsphere (MS/BUP) was prepared *via* an oil-in-water emulsion-solvent evaporation method, according to a previous protocol with minor modification [13]. Briefly, PLGA (100.0 mg) and BUP (100.0 mg) were dissolved in 2.0 mL of DCM. After complete dissolution, the solution was added dropwise to 20.0 mL of 1.5% (*W/V*) PVA aqueous solution and homogenized using a high-speed shearing machine (BME100LX, Wei Yu Mechanical and Electrical Manufacturing Co., Ltd., China) at 2,000 rpm for 2 min. The emulsion formed was immediately poured into 100.0 mL of 0.5% (*W/V*) PVA aqueous solution and stirred by using a magnetic stirrer for 6 h until the MS solidified. The MS was collected by centrifugation at 2,600 rcf for 4 min, washed with distilled water thrice to remove PVA and unentrapped drugs, and then freeze-dried for further use. The amount of BUP was determined using ultraviolet-visible (UV-vis) spectrometer (UV-1800, Shimadzu, Kyoto, Japan) at 263 nm, and the drug-loading content (DLC) was calculated by DLC (%) = W_{BUP} / $W_{MS/BUP}$ × 100%, where W_{BUP} represents the weight of BUP in MS/BUP, and $W_{MS/BUP}$ represents the weight of MS/BUP.

Preparation of BUP-entrapped Gel and Gel–microsphere

The triblock copolymer PLGA–PEG–PLGA was prepared by the ring-opening polymerization (ROP) of L-LA and GA with PEG and $Sn(Oct)_2$ as the macroinitiator and catalyst, respectively. The mass

percentage of PLGA−PEG−PLGA copolymer in the thermosensitive Gel was 20 wt.% as described previously. The sol-gel transition temperature of PLGA−PEG−PLGA polymer was related to its concentration, and when the concentration of polymer increased from 15 to 25 wt.%, the sol-gel temperature decreased from 29 to 24 °C. Therefore, PLGA−PEG−PLGA with a concentration of 20 wt.% is suitable for *in situ* drug delivery as it exhibits solution state at room temperature (25 °C) and changes rapidly to the gel state when exposed to body temperature (37 °C) [32, 33]. The BUP-entrapped PLGA−PEG−PLGA Gel (Gel−BUP) and Gel−microsphere (Gel−MS/BUP) were prepared by dissolving PLGA−PEG−PLGA copolymer and BUP or MS/BUP in phosphate-buffered saline (PBS). There was 89.0 mg MS/BUP (containing 40.0 mg BUP) in 0.6 mL of Gel−MS/BUP. The dosage of MS was according to an earlier study, which proved that PLGA MS containing 40.0 mg BUP could significantly inhibit the incisional pain in rats and showed effective postoperative analgesia [34]. In the Gel−BUP system (control group), 89.0 mg MS/BUP was replaced with 40.0 mg BUP. The samples were stirred at 4 °C for 24 h to form homogeneous suspensions. Then, the suspensions were placed in a thermostat at 37 °C for 10 min for the formation of Gel−BUP and Gel−MS/BUP.

Scanning electron microscopy characterizations

The morphologies of BUP·HCl, BUP, MS/BUP, Gel, Gel−BUP, and Gel−MS/BUP were studied by scanning electron microscopy (SEM; Philips XL30, Eindhoven, The Netherlands). The samples of Gel, Gel−BUP, and Gel−MS/BUP were pre-prepared as described above, stirred for 24 h at 4 °C and placed in a thermostat at 37 °C for 10 min for Gel formation, followed by freezing in liquid nitrogen for 30 s and lyophilization. The MS/BUP powder and Gel pieces were observed by SEM with an acceleration voltage of 10 kV.

Confocal laser scanning microscopy analyses of Gel−MS

Confocal laser scanning microscopy (CLSM) analysis was used to further investigate the relative structure of the Gel and MS in the Gel−MS system [35]. The preparation of C6-labeled MS (MS-C6) was carried out similarly to that of MS/BUP. The weight ratio of PLGA to C6 was 100:1. To prepare the RhB-labeled PLGA−PEG−PLGA (PLGA−PEG−PLGA-RhB), 1.0 g of PLGA−PEG−PLGA, 200.0 mg of RhB, and 100.0 mg of EDC·HCl were added to 5.0 mL of DMF. DMAP (4.0 mg) was added as a catalyst. The mixture was stirred at room temperature for 24 h in the dark. PLGA−PEG−PLGA-RhB was dialyzed against double-distilled water (ddH_2O) for three days to remove the unlabeled RhB. Subsequently, MS-C6 and PLGA−PEG−PLGA-RhB were lyophilized, re-dissolved in PBS, and stirred for 24 h at 4 °C. The above solution was placed in a thermostat at 37 °C for 10 min, followed by freezing in liquid nitrogen and lyophilization. The formulation was cut into sections (thickness: 20 μm) with a freezing microtome (Leica CM 1900, Wetzlar, Germany), and the slides were observed by CLSM (LSM 780, Carl Zeiss, Jena, Germany).

Rheology analyses

The rheological behaviors of the PLGA−PEG−PLGA copolymer solution without or with BUP and MS were investigated using an MCR 302 rheometer (Anton Paar, Graz, Austria) [32]. The temperature was set to 5−60 °C with temperature increments of 0.5 °C/min. Premixed samples (350.0 μL) were added to a 25.0 mm parallel plate. The samples were allowed to stand for 5 min for structure recovery before enough silicone oil was added to cover the free surface and limit dehydration. The storage modulus (G') and loss modulus (G'') were measured at a strain and frequency of 1% and 1 Hz, respectively.

In vitro release, and erosion and degradation properties

The release profiles of BUP from MS/BUP were determined by an immediate release method [36]. Briefly, the MS/BUP powder (74.0 mg) was added to 3.0 mL of PBS without or with 2.0 mg mL^{-1} of elastase. Subsequently, the centrifuge tubes were incubated in a 37 °C shaking incubator at 70 rpm. At specified intervals over a 9-day period, the upper buffer was collected after centrifugation at 2,600 rcf for 4 min. After that, an equal volume of fresh buffer was added, and the remaining MS/BUP was placed in the incubator again. To study the erosion and degradation properties of MS/BUP, preweighed MS/BUP (74.0 mg) was placed in centrifuge tubes containing 3.0 mL of PBS without or with elastase (2.0 mg mL^{-1}). The tubes were kept in a 37 °C shaking incubator at 70 rpm. At predetermined intervals, the degradation medium was removed by centrifugation, and the remaining MS/BUP were rinsed with ddH_2O, lyophilized, and weighed for degradation determination [37]. To study the release property of BUP from Gel−BUP and Gel−MS/BUP, 0.5 g of the PLGA−PEG−PLGA copolymer solution with BUP or MS/BUP was put in a cylindrical vial with a diameter of 16 mm and placed in a water bath at 37 °C until the formation of Gel−BUP or Gel−MS/BUP. Afterward,

3.0 mL of PBS without or with 2.0 mg mL^{-1} of elastase was slowly added to the surface of Gel−BUP or Gel−MS/BUP. The vials were kept in a 37 °C shaking incubator at 70 rpm. PBS was collected at predetermined intervals, and fresh buffer was added to the samples for further measurement. The concentration of BUP released into PBS was determined by measuring the absorption value at 263 nm. To evaluate the erosion and degradation properties of Gel−MS/BUP and Gel−BUP, 3.0 mL of PBS without or with elastase (2.0 mg mL^{-1}) was slowly added on the surface of Gel−MS/BUP and Gel−BUP (~0.5 g) in cylindrical vials, and the samples were placed in a 37 °C shaking incubator at 70 rpm. PBS was removed, and the remaining formulations were weighed every other day.

Animals

Male Wistar rats (250−350 g) were purchased from the Experimental Animal Center of Jilin University (Changchun, P. R. China). The animals were housed in ventilated cages with controlled temperature and humidity, under a 12-h light-dark cycle. Animals had access to rodent chow and water *ad libitum*. Five days before the experiments, the animals were handled to familiarize them with the experimental environment. All rats were handled under a protocol approved by the Institutional Animal Care and Use Committee of Jilin University.

In vivo analysis of the immobilization effect of Gel−MS system

To verify the immobilization effect of Gel on MS in Gel−MS system, NR-loaded MS (MS/NR) and Gel−MS (Gel−MS/NR) were prepared and injected to the sciatic nerve, followed by analysis of MS diffusion. MS/NR was prepared as described above, and the weight ratio of PLGA and NR was 20:1. After freeze-drying, the MS/NR (10.0 wt.%) was added into the PLGA−PEG−PLGA copolymer solution (20.0 wt.%), and the mixture was stirred at 4 °C for 24 h. Then, the suspensions of MS/NR in PBS and Gel−MS/NR were injected into the sciatic nerve at the left posterior limbs of rats (n = 3) [38]. After the animals were anesthetized with 2% isoflurane in oxygen (Sevorane™, Abbott Spa, Campoverde, Italy) and placed in a lateral position, MS/NR or Gel−MS/NR were administered *via* a 23-gauge needle. Specifically, the needle was introduced to the posteromedial of the greater trochanter and advanced in an anteromedial direction, from posteromedial and anteromedial parallel to the spine. Once the needle contacted the bone, 0.6 mL of the formulation was injected into the left posterior limb. Notably, Gel−MS/NR was administered as solution and allowed to form *in situ* Gel automatically under the stimulus of body temperature. 10 min, 10 h, 20 h, and 30 h after administration of the formulations, the rats were deeply anesthetized with 10% (*W/V*) chloral hydrate and perfused *via* the heart with normal saline and 4% (*W/V*) PBS-buffered paraformaldehyde. The muscles and sciatic nerve were exposed, and the sciatic nerve and surrounding tissue, as well as the muscles far from the injection site (0.5 and 1.0 cm) were collected, fixed with 4% (*W/V*) PBS-buffered paraformaldehyde overnight, and dehydrated with 30% (*W/V*) PBS-buffered sucrose. Then, the tissues were cut into sections with a thickness of 10 μm with a freezing microtome, and the slides were analyzed by CLSM. After that, the fluorescence intensity of NR in each group was semi-quantitatively analyzed by ImageJ software (National Institutes of Health, Bethesda, MD, USA, http://imagej.nih.gov/ij/).

Rat sciatic nerve blockade

Sciatic nerve blocking was performed by intramuscular injection. Briefly, Wistar rats were randomly divided into four groups (n = 8). After the animals were anesthetized with 2% isoflurane in oxygen (Sevorane™, Abbott Spa, Campoverde, Italy) and placed in a lateral position, 0.6 mL of (1) 3.0 mg BUP·HCl in PBS (BUP·HCl), (2) 40.0 mg BUP in Gel (Gel−BUP), (3) 40.0 mg BUP in MS (MS/BUP), and (4) 40.0 mg BUP in Gel−MS system (Gel−MS/BUP) were separately injected into the left posterior limb *via* a 23-gauge needle as described above. The right posterior limb served as an untreated control.

Assessment of neurological behavior

Sensory blockades were evaluated by a modified thermal withdrawal latency assay. Briefly, the hind paw of the experimental rat was exposed to a hot plate preheated to 56 °C, and the time until the rat lifted or licked its hind paw was recorded as thermal latency. Baseline assessments were performed on all animals for at least two days before the experiments. Normal thermal latency was about 2 s, and animals with baseline thermal latency shorter than 2 s or longer than 4 s were excluded. The maximum allowed latency was 12 s, after which the paw would be removed manually to avoid tissue injury, and a thermal withdrawal of 12 s was recorded [39]. The test was applied every hour for the first 2 h, and then every 2 h until full recovery. Each rat was evaluated thrice, alternating between the left and right hind paws, with intervals of over 30 s. The average value was taken as the thermal latency. The results were expressed as maximum percentage effect (MPE) using the equation $MPE\ (\%) = (P - B) / (C - B) \times 100\%$, where B represents the baseline thermal latency, P

represents the thermal latency response at predetermined intervals, and *C* represents the maximum allowed latency [40]. The duration from drug administration to recovery of thermal latency (<50% MPE) was considered as the nerve block duration.

Motor block was evaluated using a 4-point scale [41]. In brief, 1 point represents normal appearance; 2 points indicates intact dorsiflexion of the foot with impaired splaying of the toes when the animal is lifted by the tail; 3 points indicate plantarflexion of the foot with no ability to splay the toes; 4 points represents complete loss of dorsiflexion, plantarflexion, and an impairment in gait. The duration of motor blockade was defined as the time duration from 4 to 2 points. Additionally, tactility, proprioception, grip, and limp were also assessed as either present or absent.

Sciatic nerve dissection and histology

On day 7 and 21 post-injection, the rats were deeply anesthetized with 10% (*W*/*V*) chloral hydrate and perfused *via* the heart with normal saline and 4% (*W*/*V*) PBS-buffered paraformaldehyde [39]. The sciatic nerve and surrounding tissue were exposed, and the gross pathology was evaluated by qualitative inspection. Next, the sciatic nerve was collected with surrounding tissues, fixed with 4% (*W*/*V*) PBS-buffered paraformaldehyde overnight, and embedded in paraffin. The paraffin-embedded tissues were cut to 10 μm thickness and stained with hematoxylin & eosin (H&E). The stained slides were observed by light microscopy (Nikon TE2000U, Kanagawa, Japan), and the tissue inflammatory response was qualitatively evaluated as mild, moderate, or severe.

Immunohistochemical analyses

The degrees of tissue response of the sciatic nerve and surrounding muscles were further investigated by immunohistochemical analyses of inflammatory factors, *i.e.*, interleukin-1 (IL-1), interleukin -6 (IL-6), and tumor necrosis factor-α (TNF-α) [42, 43]. The paraffin-embedded samples were incubated at 60 °C for 2 h, followed by dewaxing in xylene twice and hydration in graded ethanol (100, 95, 80, and 75%, *V/V*). Then, the hydrated samples were washed with PBS and blocked with goat serum in a humid chamber for 30 min at 37 °C. The primary antibody solutions of IL-1, IL-6, and TNF-α (1:50 dilution; Abcam Company, Cambridge, USA) were added to the surface of the samples and incubated overnight at 4 °C. The appropriate FITC-labeled secondary antibody solution (1:50 dilution; Boster Biological Engineering Co., Ltd., Wuhan, P. R. China) was then added to the slides and incubated for 1 h at 37 °C. DAPI was used to stain the nucleus for three minutes at room temperature. The sections were observed and photographed by CLSM with an excitation wavelength of 488 nm and an emission wavelength of 525 nm. Inflammatory factors were semi-quantitatively assessed using ImageJ software.

Toluidine blue O (TBO) and TUNEL staining

After deep anesthetization, the rats were perfused through the heart with normal saline and 4% (*W*/*V*) PBS-buffered paraformaldehyde at 7 and 21 days after drug injection. The sciatic nerve was extracted, fixed in 2.5% glutaraldehyde in PBS for 24 h, fixed overnight in 1% (*W*/*V*) osmium tetroxide, dehydrated in a graded ethanol series, and finally embedded in Epon 812. Subsequently, semi-thin section (0.5 μm) was cut, stained with 0.1% (*W*/*V*) TBO, and observed under light microscopy (AxioImager A2, Carl Zeiss, Jena, Germany).

A terminal deoxynucleotidyl transferase-mediated dUTP nick-end labeling (TUNEL) assay was carried out to investigate the neurotoxicity of BUP-containing formulations. Samples were hydrated and immersed in proteinase K solution for 30 min at 37 °C, and then immersed in 3% hydrogen peroxide (H_2O_2) for 10 min and washed with PBS twice. Next, the samples were incubated in a TdT enzyme reaction solution at 37 °C for 60 min and rinsed with PBS thrice. They were immersed in streptavidin-FITC at 37 °C for 30 min and DAPI for 3 min at room temperature. Finally, they were rinsed with PBS and sealed with 30% glycerol in PBS. Apoptosis in the sciatic nerves was determined by CLSM.

Statistical analyses

All experiments were repeated thrice, and the results are expressed as mean ± standard deviation (SD). Statistical differences were evaluated with paired Student's *t*-tests in SPSS 23.0 (SPSS Inc., Chicago, IL, USA). $P < 0.05$ indicated statistical significance, and $P < 0.01$ and $P < 0.001$ were considered highly significant.

Results and discussion

Preparation and characterization of BUP

Bupivacaine is an amide local anesthetic that can reversibly block nerve conduction by acting on the voltage-gated sodium (Na^+) channels in membranes [44]. BUP passes through cell membranes more easily than BUP·HCl does because of the hydrophobicity of the lipid bilayer [45]. BUP also binds more strongly to the lipid bilayer than BUP·HCl, thereby protecting drugs from diffusing to extracellular media and the bloodstream, decreasing their elimination [46]. Therefore, the analgesic effects of local anesthetics

may be related to their hydrophobicity, which likely contributes to a faster time of onset and longer duration of effect. This factor gives BUP a significant advantage over BUP·HCl in sustained drug delivery systems.

In this study, BUP·HCl, which is a water-soluble white powder, was alkalized by adding NaOH to its saturated solution, and then the insoluble BUP was precipitated out of the water. The SEM analysis of BUP·HCl revealed large, rough-edged, and rectangular crystals with diameters of 50–100 μm. In contrast, BUP showed a flat, needle-like morphology with <1 μm dimension (**Figure 1A**). The morphology and size of the BUP prepared in this study were changed after base precipitation and showed highly anisotropic shapes, which were similar to those observed in a previous study, suggesting success of the alkali precipitation [47].

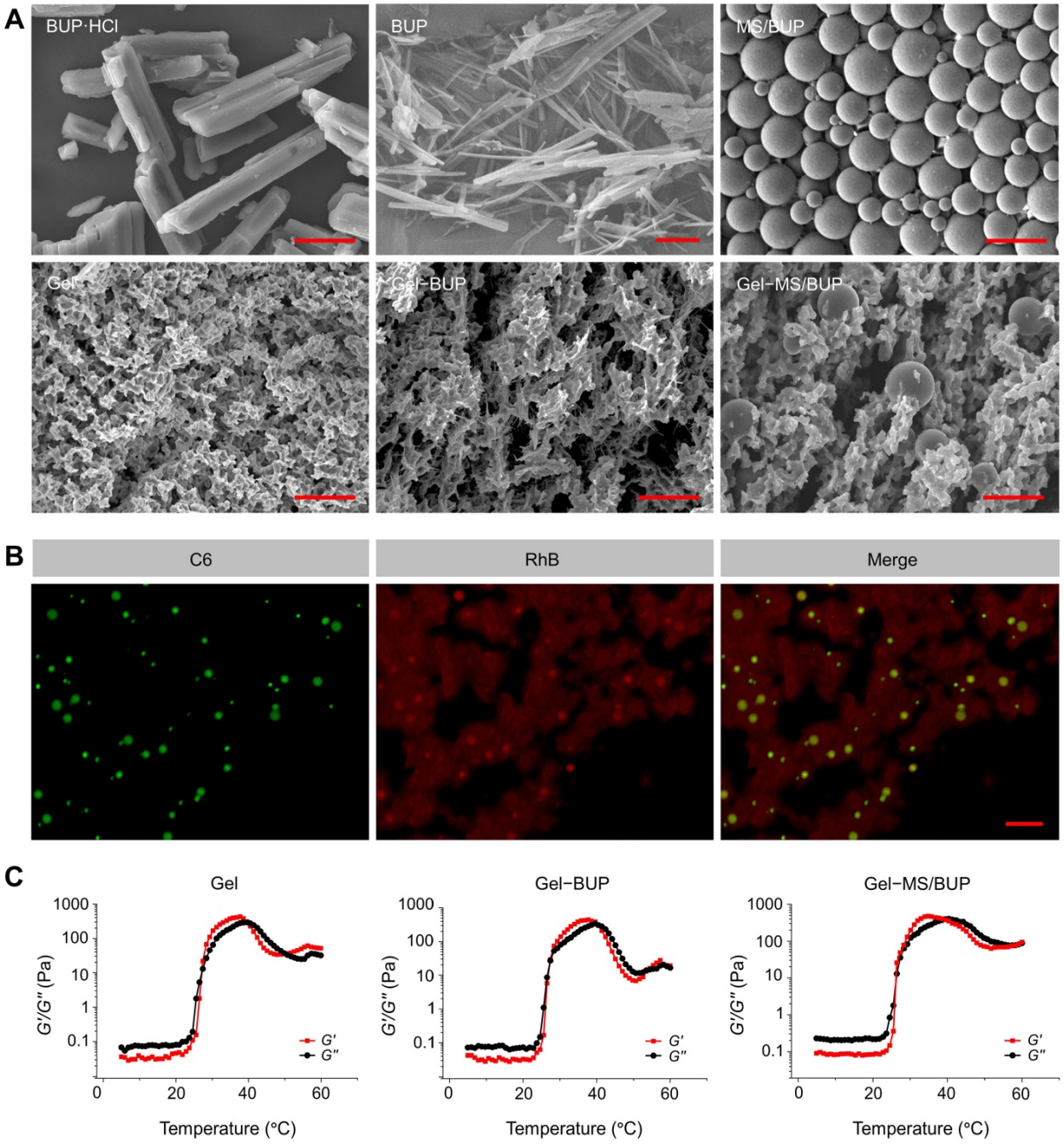

Figure 1. Characterization of the Gel–microsphere system. **(A)** SEM images of BUP·HCl, BUP, and MS (the upper panel), and Gel, Gel–BUP, and Gel–MS/BUP (the lower panel). Scale bars are 2.5 μm for BUP and 25 μm for the others. **(B)** CLSM analysis of fluorescently labeled Gel–MS. Green and red fluorescences indicate C6-labeled MS and RhB-labeled Gel, respectively. Scale bar = 100 μm. **(C)** Rheological properties of Gel, Gel–BUP, and Gel–MS/BUP.

Preparation and characterization of MS/BUP and Gel−MS/BUP

BUP-loaded PLGA MS was formulated using an emulsion-solvent evaporation method [36]. Firstly, PLGA and BUP were thoroughly dissolved in dichloromethane. After emulsification and solidification, MS/BUP was filtered to obtain an enriched population smaller than 30 μm. The morphology and size of MS/BUP were measured by SEM measurements (**Figure 1A**), and the particles exhibitied a smooth surface and spherical shape. The size distribution was homogeneous, with an average size of approximately 15 μm. UV-vis analysis estimated the DLC of MS/BUP to be approximately 45 wt.%.

The triblock copolymer PLGA−PEG−PLGA was prepared by the ring-opening polymerization (ROP) method, and the generated Gel exhibited an interconnected three-dimensional (3D) porous network structure (**Figure 1A**). When BUP was added into the Gel, the needle-like BUP was interspersed throughout the Gel matrix (**Figure 1A**).

The Gel−MS/BUP was developed by mixing MS/BUP with PLGA−PEG−PLGA solution at 4 °C for 24 h to form a homogeneous suspension. Then, the suspension was placed in a thermostat at 37 °C for 10 min to form Gel−MS/BUP. As shown in **Figure 1A**, MS was dispersed uniformly on the surface and inside the Gel matrix. Overall, the Gel−MS/BUP exhibited a well-structured and homogeneous construction with effective encapsulation of BUP and, thus, could be suitable for sustained local anesthetic delivery.

To better understand the distribution of MS in the Gel−MS system, the MS and Gel matrix were labeled with C6 and RhB, respectively, and then examined using CLSM. As shown in **Figure 1B**, when C6 was encapsulated in PLGA MS (MS-C6), strong green fluorescence was observed under excitation with a 488 nm laser [48]. To label the Gel, RhB was covalently conjugated to the PLGA−PEG−PLGA copolymer in the presence of the catalyst DMAP [49]. As shown in **Figure 1B**, MS-C6 with green fluorescence was uniformly distributed in the Gel with red fluorescence. In addition, most of the MSs were located in the matrix rather than the pores of the Gel. Thus, the Gel could effectively encase MS and promote the *in situ* sustained release of BUP.

To investigate whether the addition of BUP and MS/BUP would alter its gelation properties, the rheologic characteristics of the Gel with and without BUP or MS/BUP were evaluated. G' represents the stiffness of the sample and G'' refers to the viscosity of the sample. Compared with the blank Gel, both the initial and maximum values of G' and G'' increased following the addition of BUP and MS/BUP (**Figure 1C**). Specifically, the change of Gel−BUP was insignificant ($P = 0.105$), while that of Gel−MS group was more pronounced ($P < 0.05$). Excessive viscosity may result in difficulties during the injection process. However, in the present study, the viscosities of Gel−BUP and Gel−MS/BUP were still relatively low at 25 °C (0.063 and 0.357 Pa, respectively) despite the presence of BUP and MS/BUP, proving their syringeability [50]. Moreover, the maximum value of G' for Gel−MS/BUP was higher than 400 Pa, indicating the satisfactory stiffness of the formulations for an *in situ* drug release system [32]. The Gel, Gel−BUP, and Gel−MS/BUP groups exhibited gelation temperatures of 27.4, 27.4, and 26.5 °C, respectively. These results indicated that the addition of BUP or MS/BUP would not significantly shift the gelation temperature. Overall, the Gel−MS/BUP exhibited favorable syringeability, stiffness, and gelation capacity, proving its feasibility for parenteral administration.

The release profiles of BUP in different BUP-containing formulations are shown in **Figure 2A**. Samples were obtained periodically over nine days, and the drug content in each sample was measured using UV-vis spectroscopy. Overall, the *in vitro* release patterns of BUP from Gel−BUP and MS/BUP were biphasic, consisting of a high initial burst release followed by a more gradual release. 28.42% and 35.94% of the drug were released from MS/BUP and Gel−BUP during the first 24 h, respectively. In contrast, BUP was released at a more stable rate from the Gel−MS system, with a significantly reduced burst release ($P < 0.05$). The release curve of BUP from Gel−MS/BUP was nearly linear. Approximately 15.3% of the loaded BUP was released over the first 24 h, a significantly lower percentage than that released from MS/BUP and Gel−BUP ($P < 0.05$).

For MS/BUP, the initial burst release in the first phase was caused by the drug molecules located near or on the surface layer of the MS, which diffused out once they contacted the release medium. However, for the Gel−MS system, the rapid release of the drug dispersed in the Gel was retarded by the outer Gel matrix, which prevented the burst release [51]. In the second phase (after 24 h), a slow and constant drug release was induced by diffusion from the MS and the hydrophilic matrix of the Gel, as well as erosion and degradation of both the MS and Gel. Overall, the Gel−MS system, with its sustained and constant drug release pattern, would be highly applicable for the prolonged delivery of local anesthetics.

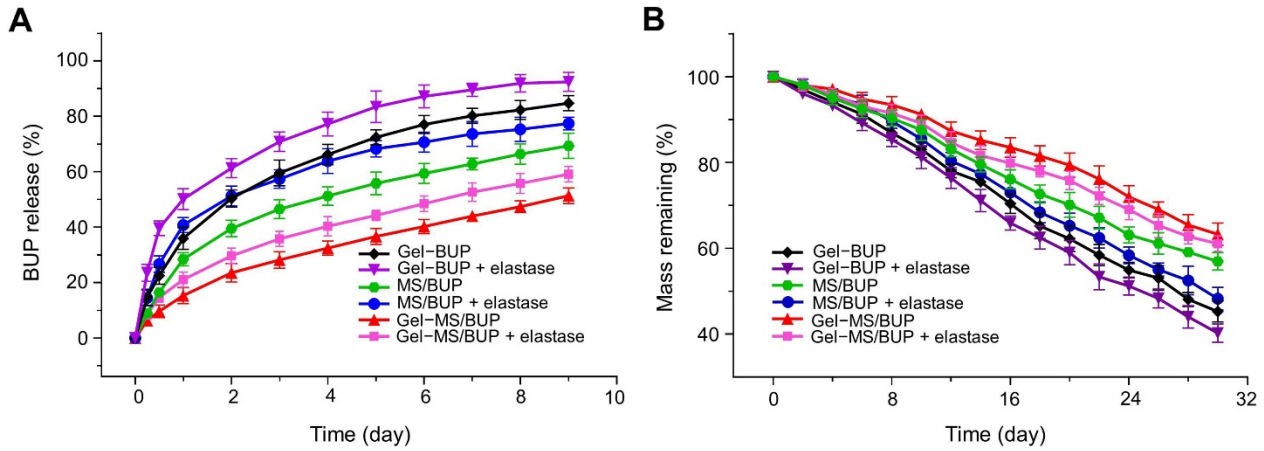

Figure 2. Drug release and degradation behaviors. **(A)** *In vitro* BUP release from Gel−BUP, MS/BUP, and Gel−MS/BUP incubated in PBS without or with elastase. **(B)** *In vitro* mass-remaining profiles of Gel−BUP, MS/BUP, and Gel−MS/BUP incubated in PBS without or with elastase.

The BUP release was accelerated by the addition of enzymes in all the formulation groups (**Figure 2A**). In total, 40.2%, 56.0%, and 50.9% of BUP were released from MS/BUP, Gel−BUP, and Gel−MS/BUP, respectively, within the first 24 h. Thus, it was expected that both the release rate and the degree of burst release could be accelerated by the presence of enzymes in the *in vivo* microenvironment. In addition, the drug content in MS, the MS amount in Gel−MS system, and the copolymer concentration of the Gel may be important factors affecting the drug release behavior because, in the Gel−MS system, the gel matrix can not only immobilize the MS but also entrap the drug molecules released from the MS and prolong the release profile. When the drug content in MS and the MS amount in Gel−MS system increase or the concentration of Gel decreases, the external Gel layer of the double-barrier release system is relatively reduced, and the drug would be released faster with a more obvious initial burst release [52-54]. The Gel−MS system in this study exhibited sustained and constant drug release without burst release. Thus, the current proportion of MS to Gel chosen in this study is suitable for sustained drug delivery. As shown in **Figure 2B**, the *in vitro* erosion and degradation assessments were consistent with those of the drug release experiments. Gel−BUP displayed the fastest erosion and degradation rate, followed by MS/BUP and Gel−MS/BUP. The erosion and degradation rates were accelerated in all groups when enzymes were added.

Compared with the conventional MS drug delivery system, the Gel−MS system should be able to immobilize the microsphere around the injection site and avoid unexpected particle diffusion. To evaluate the particle immobilization effect of Gel−MS system, fluorescently labeled MS or Gel−MS were injected to the sciatic nerve, and the distribution of MS was analyzed by CLSM. As shown in **Figure 3A**, at 10 min post injection, MSs were scattered all over the muscles rather than gathered ground the sciatic nerve in the MS/NR group, and a large number of MSs diffused to the distant muscles along the intermuscular space. In contrast, in the Gel−MS/NR group, most of the MSs gathered around the sciatic nerve, and there was almost no MS distributed in the distant muscles, which proved the immobilization effect of Gel to the MS. This phenomenon could be explained by the rapid diffusion of MS/NR along the intermuscular space, which remained suspended after injection. However, when Gel−MS/NR was injected, the micelles transformed to a viscous gel promptly and formed an *in situ* depot, which immobilized the MSs and prevented their diffusion. At 10, 20, and 30 h post injection, the distribution of MS did not change significantly, and the MS in Gel−MS/NR groups still gathered well around the sciatic nerve, indicating that the immobilization effect of the Gel in this system was durable and stable.

Semi-quantitative statistical results of fluorescence intensities are shown in **Figure 3B**. At 10 min post injection, for the MS/NR group, the fluorescence intensities of the MS around the sciatic nerve and in the muscles 0.5 and 1.0 cm from the injection site were 1.50 ± 0.22, 1.02 ± 0.20, and 0.62 ± 0.10, respectively, indicating that a large part of the MSs leaked out from the injection site. However, the fluorescence intensity of the Gel−MS/NR group in the distant muscle gap 0.5 and 1.0 cm from the injection site were 0.15 ± 0.05 and 0.06 ± 0.04, which were significantly lower than that of the MS/NR group ($P < 0.001$), demonstrating that the MS was immobilized *in situ* effectively by the Gel−MS/NR system. At 30 h post injection, the fluorescence intensities of the Gel−MS/NR group in the distant muscles were still weak (0.06 ± 0.05, 0.03 ± 0.02, and 0.05 ± 0.02), proving the immobilization effect of Gel in Gel−MS/NR system within 30 h. However, the fluorescence

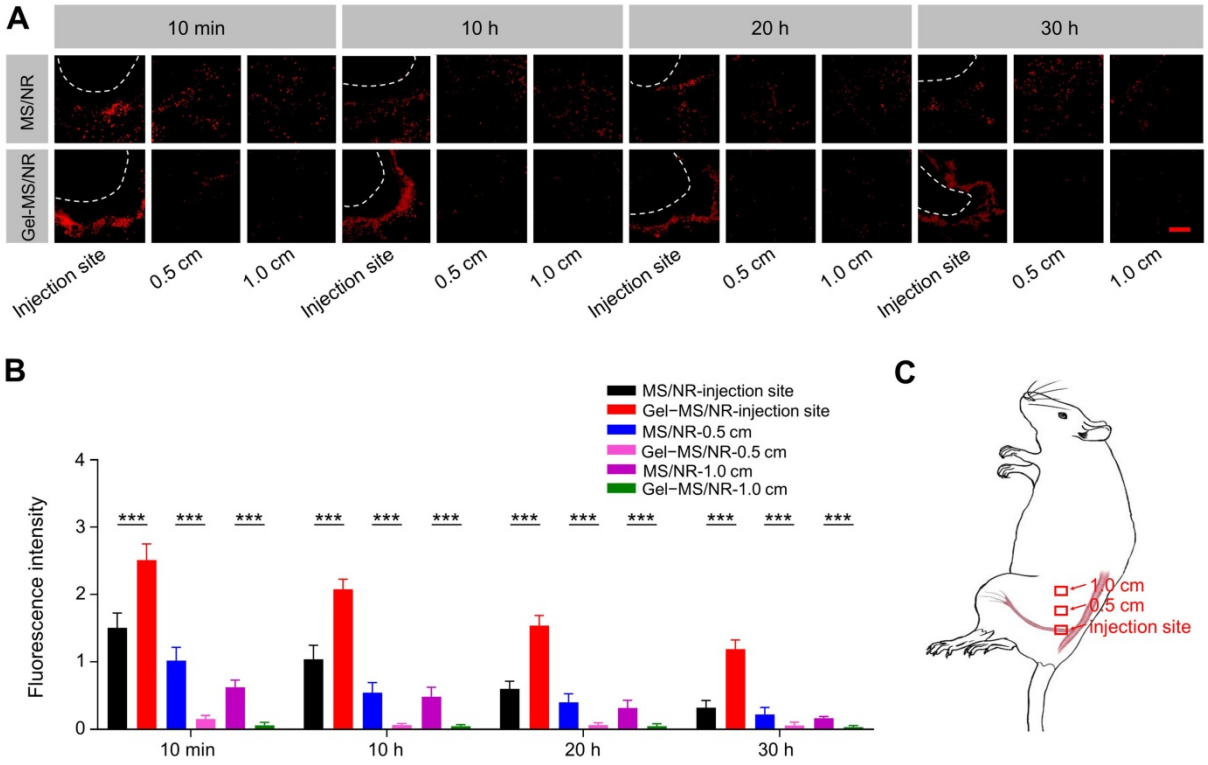

Figure 3. Immobilization effect analyses of Gel to MS. **(A)** Qualitative analysis of MS in injection site and distant muscle (0.5 and 1.0 cm from the injection site). Tissues in the injection site and distant muscles were collected 10 min, 10 h, 20 h, and 30 h post-injection. Red fluorescence indicates the NR-entrapped MS. The white dotted line represents the edge of the sciatic nerve. Scale bar = 100 μm. **(B)** Semi-quantitative analyses of fluorescence intensity in sections. Data are presented as means ± SD (n = 3; *P < 0.05, **P < 0.01, and ***P < 0.001). **(C)** Diagrammatic drawing of sampling sites.

intensities of the MS/NR in the distant muscle were 1.3 ± 0.11, 0.99 ± 0.86, and 0.72 ± 0.08, which were much higher than that of the Gel−MS group (P < 0.001). These results indicated that a large portion of the drug in the MS formulation would be distributed in the distant muscles rather than in the sciatic nerve, so it was difficult for MS only to achieve *in situ* release of drug for a long period. On the other hand, compared with MS/NR, the Gel−MS system exhibited much better *in situ* property, and MS was firmly immobilized around the sciatic nerve to form an *in situ* depot for long-term drug delivery without local diffusion.

In vivo sciatic nerve blockade

To detect the intensity and duration of the sciatic nerve blockade, the BUP-containing formulations were injected into the sciatic nerve, and neurobehavioral testing was carried out. In the sensory testing, the thermal withdrawal latency was measured, and the local anesthetic effect was expressed as MPE. The duration of analgesia was calculated from drug injection to 50% MPE. For all the BUP-containing formulations, the maximum allowed latency was obtained in the first 10 min post-injection, confirming the fast onset despite the sustained release of BUP. MPE of the BUP·HCl group returned to baseline at 2 h after treatment (**Figure 4A**), whereas the MPE of animals injected with MS/BUP, Gel−BUP, and Gel−MS/BUP remained at 100%. The MPEs of the MS/BUP and Gel−BUP groups started to decrease at 18 h post-injection, which was remarkably faster than that of the Gel−MS/BUP group at 22 h. In this work, BUP·HCl was used as a control group instead of BUP because BUP is water insoluble and BUP·HCl is widely used in the clinic.

Animals treated with Gel−BUP, MS/BUP, and Gel−MS/BUP presented sensory blockades lasting for 19 ± 1.52, 19.75 ± 1.28, and 24.25 ± 1.28 h, respectively (**Figure 4C**), which were significantly longer than that induced by BUP·HCl, *i.e.*, 2.25 ± 0.71 h (P < 0.001). Therefore, incorporation of BUP into Gel, MS, or Gel−MS could significantly enhance its analgesic effect (P < 0.001). Moreover, compared with Gel−BUP and MS/BUP, Gel−MS/BUP showed a longer duration of sensory blockade and recovered more slowly.

The stepwise release mechanism of the Gel−MS system enabled it to provide a constant BUP release over a longer period without burst release, ensuring local drug concentration and long-term nerve block. Furthermore, as a thermosensitive Gel, the liquid PLGA−PEG−PLGA copolymer solution rapidly transformed into Gel after injection. We believe that the *in situ* Gel prevented the diffusion of MS from the

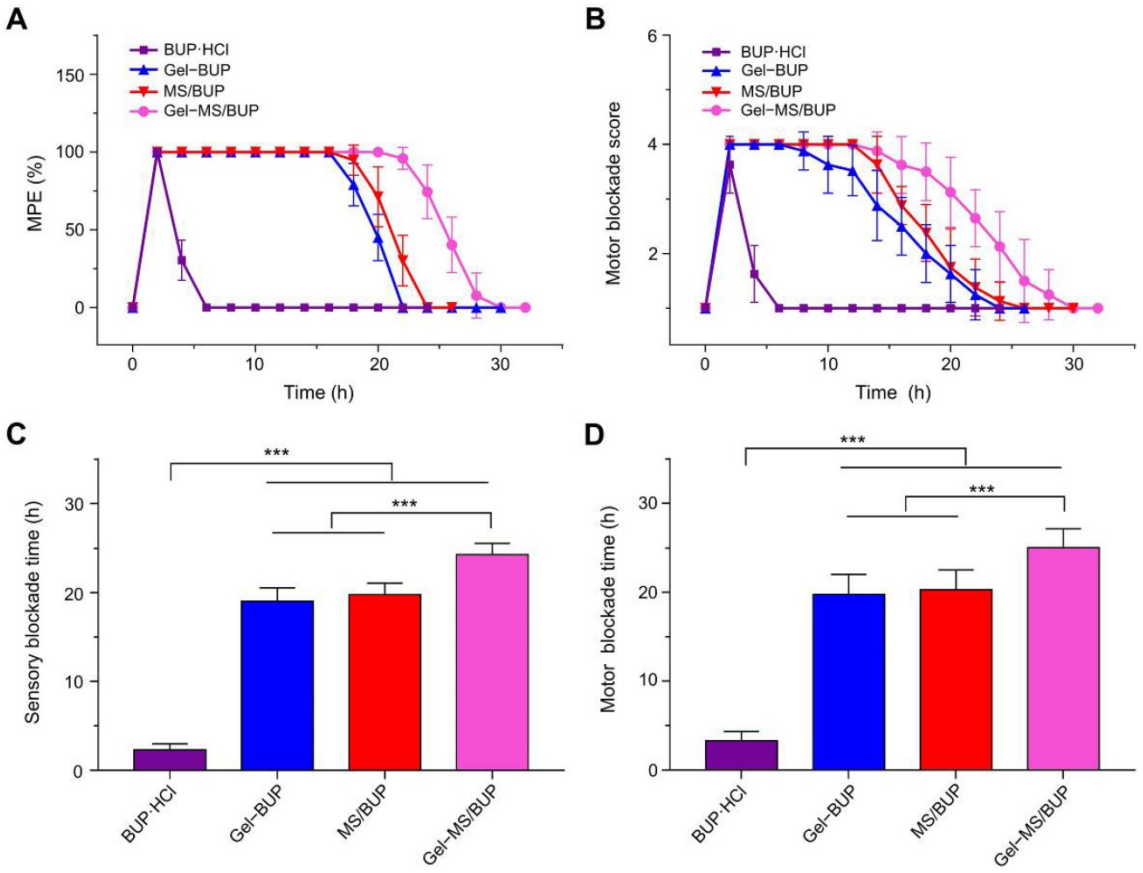

Figure 4. Sciatic nerve blockade effect. **(A)** MPEs of modified hot plate test after injection of different BUP-containing formulations. **(B)** Composite motor blockade scores for rats injected with different BUP-containing formulations. **(C-D)** Sensory and motor blockade durations after injection of different BUP-containing formulations. Data are shown as mean ± SD (n = 8; *P < 0.05, **P < 0.01, and ***P < 0.001).

injection site, thus providing adequate drug concentration around the sciatic nerve, which is important for long-acting drug delivery. Furthermore, the Gel increased the injectability of the MS, ensuring their penetration through the syringe needle, and avoiding syringe obstruction and accumulation of MS residues after injection. It could be speculated that this improvement in injectability might increase the accuracy of injection and the injected dosage of formulations, which may further improve the nerve blocking effect to a certain extent. No statistically significant differences were observed between Gel−BUP and MS/BUP in sensory blockade duration, although the former had a slower drug release curve. This might be related to the *in situ* properties of the Gel, which caused the local release of BUP around the sciatic nerve.

A functional motor blockade score was determined simultaneously with the sensory measurement. Complete motor blockade also occurred in all groups following treatment, and animals treated with Gel−MS/BUP displayed the longest duration of motor blockade. Motor blockade results were roughly similar to those of sensory blockade for all of the formulations, which did not show an excessive blockade course compared with the sensory blockade (**Figure 4B, D**). To be conducive to clinical applications, it is extremely important that variation trends for sensory and motor blocks are similar for sustained-release depots.

The right hind limbs of the animals were also tested for the systemic toxicity of BUP [55, 56]. It was found that the sensory and motor block did not occur throughout the processes in the right hind limbs. This result suggests that the treatments did not induce systemic toxicity, despite the prolonged duration of nerve block. Systemic toxicity is a typical side effect of local anesthetics, and it may also cause neuro and cardiac toxicity. It is a potentially fatal condition for patients that receive local treatments of anesthetics, and anesthesiologists should understand the risks, adequately prevent, and effectively manage it [57]. No systemic toxicity was observed in any of the groups in our study, suggesting that they are safe for drug delivery.

The dosage of Gel−MS system injected to the body can influence the release kinetics of local drug delivery system, and formulation with higher dosage could bring about a faster (or larger amount of) drug release [58, 59]. The release of a moderate amount of

drug could obtain satisfactory clinical effects, while superfluous or insufficient drugs may lead to drug toxicity and side effects. The dosage used in our present study was 0.6 mL with 89.0 mg MS/BUP (40.0 mg BUP) according to the previous literature [34]. This dosage of Gel−MS/BUP in our study achieved long-term sensory and motor blockade, without contralateral nerve block or signs of systemic toxicity. Therefore, it was suitable for postoperative long-term analgesia.

Sciatic nerve dissection and tissue compatibility evaluation

Biocompatibility is of great importance for the clinical application of biomaterial formulations [60-62]. To evaluate the tissue response of BUP-containing formulations, the rats were euthanized at 7 and 21 days post-injection, and the sciatic nerves with the surrounding muscles were collected. From the gross dissection (**Figure 5A**), it was observed that all the BUP-containing formulations remained attached to the sciatic nerve on day 7 and 21, while a comparatively small amount of residue was observed on day 21 compared to that on day 7. These results demonstrated the biodegradability of the formulations, which had considerably degraded within 21 days. Some adherence of the tissues, possibly related to tissue inflammation, was found, but this was markedly relieved by day 21. Furthermore, it was observed that in some animals injected with MS/BUP, residues were not present at the injection site, but were extended to the subcutaneous tissue or distributed along the muscle gap. In contrast, this phenomenon was not observed in the Gel−BUP and Gel−MS/BUP groups. This suggested that the addition of Gel to the BUP-containing formulations could prevent the diffusion of MS from the injection site, which improved the analgesic effect and reduced the side effects.

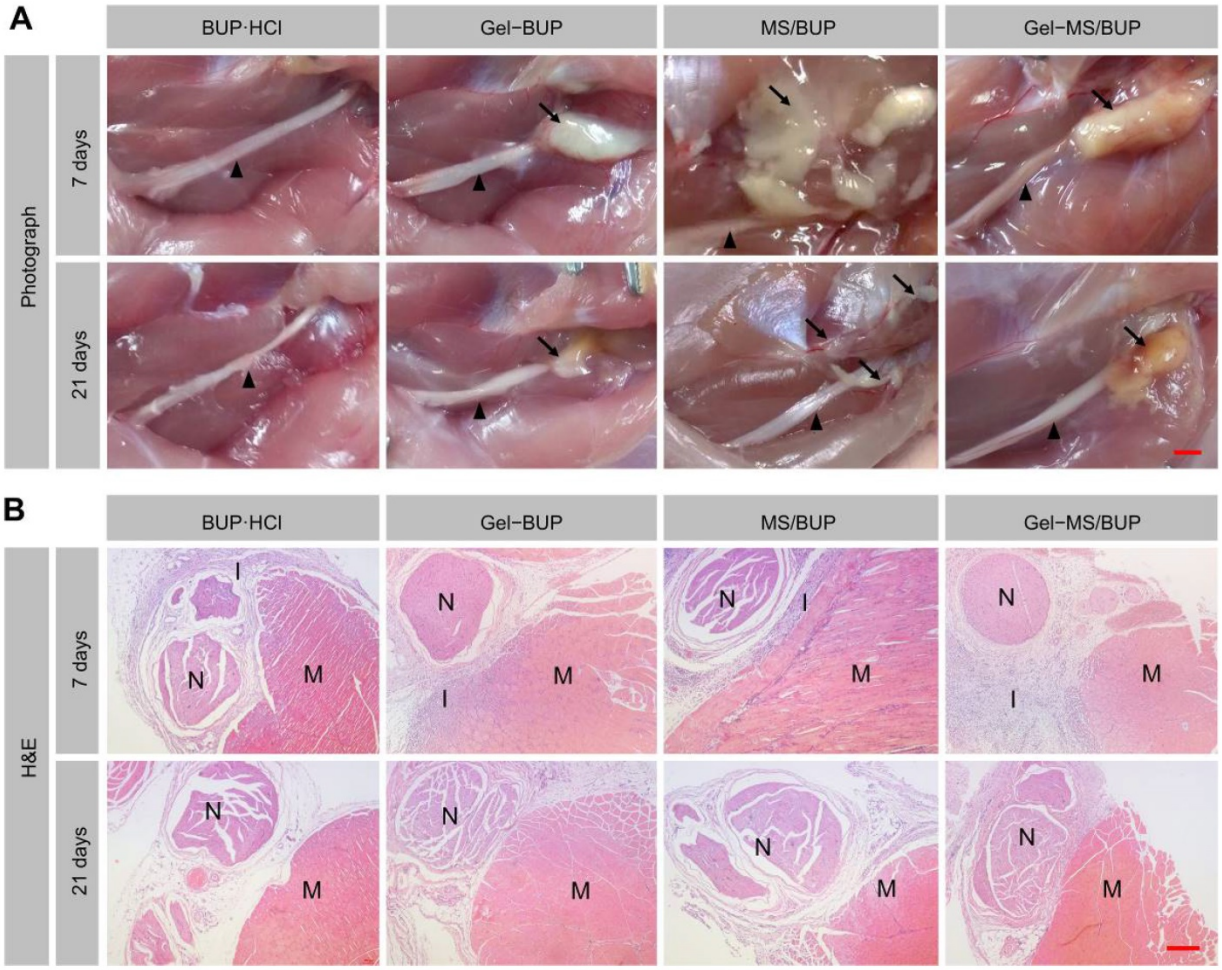

Figure 5. Gross pathology and histopathology. **(A)** Representative images of residues of BUP-containing formulations acquired 7 and 21 days after injection. Black triangle = sciatic nerve, black arrow = residue. **(B)** Representative H&E sections of the sciatic nerve and surrounding muscles. N = sciatic nerve, M = muscle, I = inflammation. The scale bars in the gross pathology panel and H&E staining panel are 5 mm and 250 μm, respectively.

The microscopic investigation of H&E-stained samples revealed that all the groups showed a certain level of inflammation on day 7. As shown in **Figure 5B**, the sustained release formulation-treated groups showed mid-level inflammation, whereas only mild inflammation was detected in the BUP·HCl group. The tissue reactions caused by the sustained release formulations might have been due to the burst or sustained release of the drug and the acid formed from the degradation of the polymer. However, such reactions are usually reversible and do not induce permanent damage [63]. Macrophages and lymphocytes were the predominant inflammatory cells, and inflammation was primarily observed in the soft tissue attached to the residues, with little inflammation evident in the nerve and muscle. In some sections of the MS group, inflammation was detected in the muscle because of MS diffusion. Moreover, 21 days post-injection, minimal inflammation was observed, indicating the reversibility of inflammatory response caused by the BUP-containing formulations.

To further assess the inflammatory response caused by the BUP-containing formulations, *in vitro* immunohistochemical staining of inflammatory factors (IL-1, IL-6, and TNF-α) was performed. Tissue response and inflammation are primarily caused by the activation of inflammatory cells. IL-1, IL-6, and TNF-α are proinflammatory cytokines produced by monocytes and macrophages. The expression of cytokines not only reflects the presence and intensity of the inflammation reaction, but also plays an important role in tissue damage and chronic pain. Therefore, these cytokines are attractive markers to estimate the tissue responses to the sustained release formulations [64].

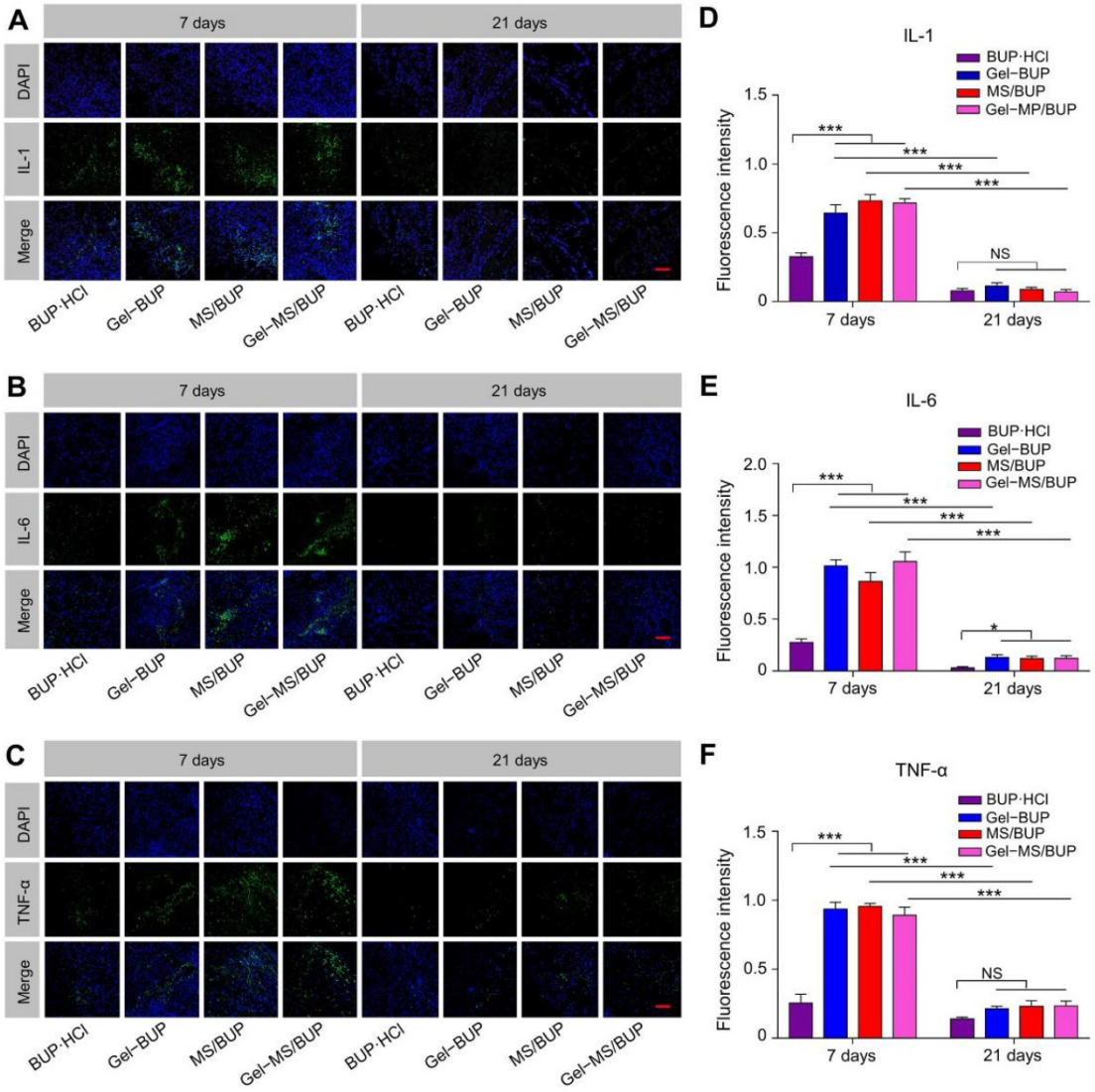

Figure 6. Qualitative and semi-quantitative analyses of inflammatory factors. **(A–C)** IL-1, IL-6, and TNF-α staining of sciatic nerve and surrounding muscles for evaluation of inflammatory response 7 and 21 days post-injection. Green fluorescence indicates the inflammatory factors, and blue fluorescence represents the nuclei. Scale bar = 100 μm. **(D–F)** Semi-quantitative analyses of fluorescence intensity in sections stained for IL-1, IL-6, and TNF-α. Data are presented as mean ± SD (n = 3; *P < 0.05, **P < 0.01, and ***P < 0.001).

The CLSM images and semi-quantitative statistical analyses of fluorescence intensities of the inflammatory factors are shown in **Figure 6**. Seven days after treatment, the green fluorescence representing the inflammatory factors labeled with FITC was observed mainly in the soft tissue around the vessels. The fluorescence in the BUP·HCl group was stronger than that of the other groups, indicating that the sustained formulations caused greater inflammatory responses than the standard formulation. However, the green fluorescence was significantly reduced in all the groups after 21 days and displayed similar intensities among the groups ($P < 0.05$), suggesting a reversal of inflammation (**Figure 6A-C**). As shown in **Figure 6D-F**, fluorescence intensities of the groups treated with Gel−MS/BUP on day 7 were 0.72 ± 0.03, 1.05 ± 0.09, and 0.89 ± 0.06 for IL-1, IL-6, and TNF-α, respectively, which were not significantly different from those of MS (0.73 ± 0.05, 0.86 ± 0.09, and 0.96 ± 0.02 for IL-1, IL-6, and TNF-α, respectively) and Gel (0.64 ± 0.06, 1.01 ± 0.06, and 0.94 ± 0.05 for IL-1, IL-6, and TNF-α, respectively). Moreover, the fluorescence intensities in these groups were significantly higher than those of animals treated with BUP·HCl, *i.e.*, 0.33 ± 0.03, 0.28 ± 0.04, and 0.25 ± 0.07 for IL-1, IL-6, and TNF-α, respectively ($P < 0.001$). The upregulation of inflammatory factors indicated the existence of tissue response. The inflammatory response observed was moderate, showing negligible green fluorescence in most areas. Consistent with the H&E staining, the semi-quantitative values of the inflammatory factors in the experimental groups were significantly reduced at 21 days post-injection ($P < 0.001$). There were no statistical differences between these groups, except that the value of TNF-α in the BUP·HCl group was lower than those in all the other groups ($P < 0.05$). These results suggested that the inflammatory response to the formulations was reversible and decreased gradually over time, which is a highly desirable quality for drug delivery applications.

Considering that H&E staining is not sensitive in detecting neurotoxicity, nerve tissues at 7 and 21 days post-injection were processed for TBO staining and TUNEL staining procedures. In all groups, the nerve fibers were regularly and compactly arranged and

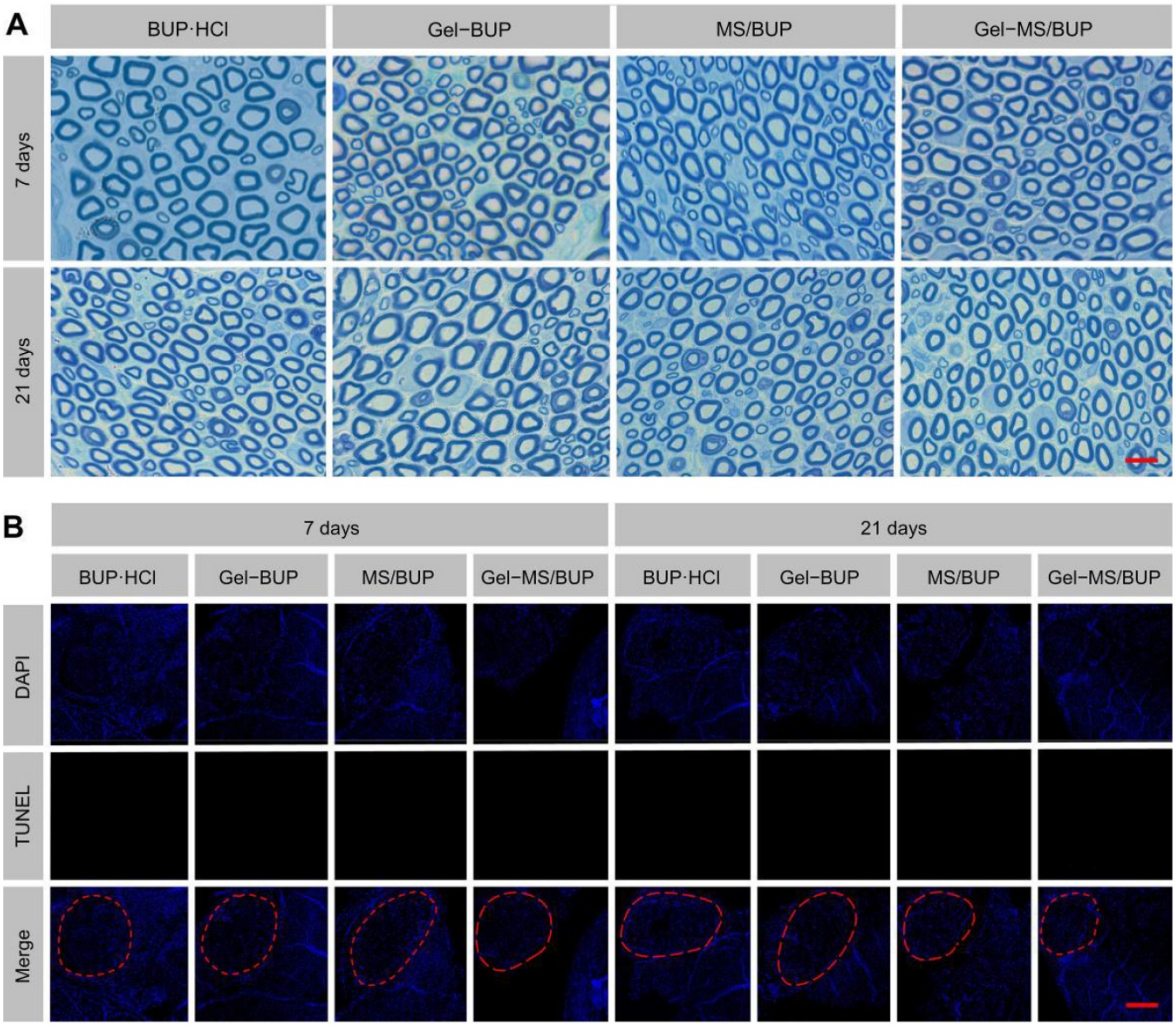

Figure 7. Determination of neurotoxicity. **(A)** TBO staining. Scale bar = 10 μm. **(B)** TUNEL staining. The red circles indicate sciatic nerves. Scale bar = 100 μm.

surrounded by rounded or elliptical myelin sheaths (**Figure 7A**). The density of the axonal elements and the structure of myelin did not change in any of the groups. The results indicate that the applications of BUP-containing formulations did not damage the nerve fiber structure. A previous study also confirmed the safety of a sustained release formulation, by discovering that it did not cause morphological changes to the sciatic nerve [39]. Apoptosis is thought to be an important cause of the neurotoxicity of local anesthetics and may be related to the p38 mitogen-activated protein kinase (MAPK) pathway [65]. As shown in **Figure 7B**, no TUNEL-positive cells were observed, indicating that no apoptosis occurred in any of the groups. Collectively, the results of TBO and TUNEL staining indicate that the tested formulations are ideal for local anesthetic applications without neurotoxicity.

Conclusion

Pain management with local anesthetics is usually limited by the short duration of analgesia. Encapsulating local anesthetics in a sustained release system provides sustained drug release and thereby increases the duration of analgesia after a single injection. In this study, an injectable Gel−MS system consisting of *in situ* thermosensitive PLGA−PEG−PLGA Gel and BUP-loaded PLGA MS was fabricated. The MS/BUP in this system was immobilized by the Gel and exhibited excellent local retention characteristics; thus, a precision-guided drug release and retention system was achieved and exhibited prolonged effective analgesia *in vivo*. Collectively, this precision-guided long-acting analgesia system, which could provide sufficient postoperative pain relief without side effects in a rat sciatic nerve block model, has great potential to be used as an alternative for clinical pain management.

Abbreviations

3D: three-dimensional; BUP: bupivacaine free base; BUP·HCl: bupivacaine hydrochloride; C6: coumarin 6; CLSM: confocal laser scanning microscopy; DAPI: 4′,6-diamidino-2-phenylindole dihydrochloride; DCM: dichloromethane; ddH_2O: double-distilled water; DLC: drug-loading content; DMAP: dimethyl aminopyridine; DMF: dimethyl formamide; EDC·HCl: 1-(3-dimethylaminopropyl)-3-ethylcarbodiimide hydrochloride; *G*′: storage modulus; *G*″: loss modulus; GA: glycolide; Gel−MS: Gel−microsphere; Gel−MS/NR: Nile red-loaded Gel−microsphere; H&E: hematoxylin & eosin; H_2O_2: hydrogen peroxide; IL-1: interleukin-1; IL-6: interleukin -6; L-LA: L-Lactide; MAPK: mitogen-activated protein kinase; MPE: maximum percentage effect; MS/BUP: bupivacaine-loaded microsphere; MS/C6: coumarin 6-loaded microsphere; MS/NR: nile red-loaded microsphere; NaOH: sodium hydroxide; NR: Nile red; PLGA: poly(lactic-*co*-glycolic acid); PLGA−PEG−PLGA: poly(lactic acid-co-glycolic acid)-*block*-poly(ethylene glycol)-*block*-poly(lactic acid-*co*-glycolic acid); PLGA−PEG−PLGA-RhB: rhodamine B-labeled PLGA−PEG−PLGA; PNB: peripheral nerve blockade; PVA: poly(vinyl alcohol); RhB: rhodamine B; ROP: ring-opening polymerization; SEM: scanning electron microscopy; $Sn(Oct)_2$: stannous octoate; TBO: Toluidine blue O; TNF-α: tumor necrosis factor-α; TUNEL: terminal deoxynucleotidyl transferase-mediated dUTP nick-end labeling; UV-vis: ultraviolet-visible.

Acknowledgements

This study was financially supported by grants from the National Natural Science Foundation of China (Grant Nos. 51673190, 51603204, 51673187, 51390484, 51473165, and 51520105004) and the Science and Technology Development Program of Jilin Province (Grant Nos. 20160204015SF and 20160204018SF).

Competing Interests

The authors have declared that no competing interest exists.

References

1. Foley PL, Ulery BD, Kan HM, Burks MV, Cui Z, Wu Q, et al. A chitosan thermogel for delivery of ropivacaine in regional musculoskeletal anesthesia. Biomaterials. 2013; 34: 2539−46.
2. Chou R, Gordon DB, de Leon-Casasola OA, Rosenberg JM, Bickler S, Brennan T, et al. Management of postoperative pain: A clinical practice guideline From the American Pain Society, the American Society of Regional Anesthesia and Pain Medicine, and the American Society of Anesthesiologists' Committee on Regional Anesthesia, Executive Committee, and Administrative Council. J Pain. 2016; 17: 131−57.
3. Joshi G, Gandhi K, Shah N, Gadsden J, Corman SL. Peripheral nerve blocks in the management of postoperative pain: Challenges and opportunities. J Clin Anesth. 2016; 35: 524−9.
4. Zorzetto L, Brambilla P, Marcello E, Bloise N, De Gregori M, Cobianchi L, et al. From micro- to nanostructured implantable device for local anesthetic delivery. Int J Nanomed. 2016; 11: 2695−709.
5. Morgalla M, Fortunato M, Azam A, Tatagiba M, Lepski G. High-resolution three-dimensional computed tomography for assessing complications related to intrathecal drug delivery. Pain Physician. 2016; 19: E775−80.
6. Santamaria CM, Woodruff A, Yang R, Kohane DS. Drug delivery systems for prolonged duration local anesthesia. Mater Today. 2017; 20: 22−31.
7. Ni Q, Chen W, Tong L, Cao J, Ji C. Preparation of novel biodegradable ropivacaine microspheres and evaluation of their efficacy in sciatic nerve block in mice. Drug Des, Dev Ther. 2016; 10: 2499.
8. Sivakumaran D, Maitland D, Oszustowicz T, Hoare T. Tuning drug release from smart microgel–Gel composites *via* cross-linking. J Colloid Interface Sci. 2013; 392: 422−30.
9. Kim T, Seol DR, Hahm SC, Ko C, Kim EH, Chun K, et al. Analgesic effect of intra-articular injection of temperature-responsive Gel containing bupivacaine on osteoarthritic pain in rats. BioMed Res Int. 2015; 2015: 812949.
10. Ramos Campos EV, Silva de Melo NF, Guilherme VA, de Paula E, Rosa AH, de Araújo DR, et al. Preparation and characterization of poly(ε-caprolactone) nanospheres containing the local anesthetic lidocaine. J Pharm Sci. 2013; 102: 215−26.

11. Burbridge M, Jaffe RA. Exparel (R): A new local anesthetic with special safety concerns. Anesth Analg. 2015; 121: 1113−4.
12. Rodrigues da Silva GH, Ribeiro LNM, Mitsutake H, Guilherme VA, Castro SR, Poppi RJ, et al. Optimised NLC: A nanotechnological approach to improve the anaesthetic effect of bupivacaine. Int J Pharm. 2017; 529: 253−63.
13. Andhariya JV, Shen J, Choi S, Wang Y, Zou Y, Burgess DJ. Development of *in vitro-in vivo* correlation of parenteral naltrexone loaded polymeric microspheres. J Controlled Release. 2017; 255: 27−35.
14. Belz JE, Kumar R, Baldwin P, Ojo NC, Leal AS, Royce DB, et al. Sustained release talazoparib implants for localized treatment of BRCA1-deficient breast cancer. Theranostics. 2017; 7: 4340−9.
15. Liu J, Lv X. The pharmacokinetics and pharmacodynamics of lidocaine-loaded biodegradable poly(lactic-*co*-glycolic acid) microspheres. Int J Mol Sci. 2014; 15: 17469−77.
16. Ohri R, Blaskovich P, Wang JC-F, Pham L, Nichols G, Hildebrand W, et al. Prolonged nerve block by microencapsulated bupivacaine prevents acute postoperative pain in rats. Reg Anesth Pain Med. 2012; 37: 607−15.
17. Ratajczak-Enselme M, Estebe J, Dollo G, Chevanne F, Bec D, Malinovsky J, et al. Epidural, intrathecal and plasma pharmacokinetic study of epidural ropivacaine in PLGA-microspheres in sheep model. Eur J Pharm Biopharm. 2009; 72: 54−61.
18. Kwon SK, Kim HB, Song JJ, Cho CG, Park SW, Choi JS, et al. Vocal fold augmentation with injectable polycaprolactone microspheres/Pluronic F127 Gel: Long-term *in vivo* study for the treatment of glottal insufficiency. PloS ONE. 2014; 9: e85512.
19. Chen P, Kohane D, Park Y, Bartlett R, Langer R, Yang V. Injectable microparticle-gel system for prolonged and localized lidocaine release. II. *In vivo* anesthetic effects. J Biomed Mater Res, Part A. 2004; 70: 459−66.
20. Chen X, Chen J, Li B, Yang X, Zeng R, Liu Y, et al. PLGA-PEG-PLGA triblock copolymeric micelles as oral drug delivery system: *In vitro* drug release and *in vivo* pharmacokinetics assessment. J Colloid Interface Sci. 2017; 490: 542−52.
21. Li X, Chen L, Lin H, Cao L, Cheng Ja, Dong J, et al. Efficacy of poly(D,L-lactic acid-*co*-glycolic acid)-poly(ethyleneglycol)-poly(D,L-lactic acid-*co*-glycolic acid) thermogel as a barrier to prevent spinal epidural fibrosis in a postlaminectomy rat model. Clin Spine Surg. 2017; 30: E283−90.
22. Garner J, Davidson D, Eckert GJ, Barco CT, Park H, Park K. Reshapable polymeric Gel for controlled soft-tissue expansion: *In vitro* and *in vivo* evaluation. J Controlled Release. 2017; 262: 201−11.
23. Yu S, Zhang D, He C, Sun W, Cao R, Cui S, et al. Injectable thermosensitive polypeptide-based CDDP-complexed Gel for improving localized antitumor efficacy. Biomacromolecules. 2017; 18: 4341−8.
24. Lu Y, Aimetti AA, Langer R, Gu Z. Bioresponsive materials. Nat. Rev. Mater. 2017; 2: 16075.
25. Alexander A, Ajazuddin n, Khan J, Saraf S, Saraf S. Poly(ethylene glycol)-poly(lactic-*co*-glycolic acid) based thermosensitive injectable Gels for biomedical applications. J Controlled Release. 2013; 172: 715−29.
26. Li RX, Liang JM, He YW, Qin J, He HN, Lee S, et al. Sustained release of immunosuppressant by nanoparticle-anchoring Gel scaffold improved the survival of transplanted stem cells and tissue regeneration. Theranostics. 2018; 8: 878−93.
27. Shamloo A, Sarmadi M, Aghababaie Z, Vossoughi M. Accelerated full-thickness wound healing *via* sustained bFGF delivery based on a PVA/chitosan/gelatin Gel incorporating PCL microspheres. Int J Pharm. 2017; 537: 278−89.
28. Romić M, Klarić M, Lovrić J, Pepić I, Cetina-Čižmek B, Filipović-Grčić J, et al. Melatonin-loaded chitosan/Pluronic® F127 microspheres as *in situ* forming Gel: An innovative antimicrobial wound dressing. Eur J Pharm Biopharm. 2016; 107: 67−79.
29. Fedorchak MV, Conner IP, Schuman JS, Cugini A, Little SR. Long term glaucoma drug delivery using a topically retained gel/microsphere eye drop. Sci Rep. 2017; 7: 8639.
30. Taraballi F, Minardi S, Corradetti B, Yazdi IK, Balliano MA, Van Eps JL, et al. Potential avoidance of adverse analgesic effects using a biologically "smart" Gel capable of controlled bupivacaine release. J Pharm Sci. 2014; 103: 3724−32.
31. Dinh VV, Suh YS, Yang HK, Lim YT. Spatiotemporal programing for the on-demand release of bupivacaine based on an injectable composite Gel. J Pharm Sci. 2016; 105: 3634−44.
32. Zhang Y, Ding J, Sun D, Sun H, Zhuang X, Chang F, et al. Thermogel-mediated sustained drug delivery for *in situ* malignancy chemotherapy. Mater Sci Eng C. 2015; 49: 262−8.
33. Ma H, He C, Cheng Y, Li D, Gong Y, Liu J, et al. PLK1shRNA and doxorubicin co-loaded thermosensitive PLGA-PEG-PLGA Gels for osteosarcoma treatment. Biomaterials. 2014; 35: 8723−34.
34. Ohri R, Wang JC-F, Blaskovich PD, Pham LN, Costa DS, Nichols GA, et al. Inhibition by local bupivacaine-releasing microspheres of acute postoperative pain from hairy skin incision. Anesth Analg. 2013; 117: 717−30.
35. Kong B, Zhu A, Ding C, Zhao X, Li B, Tian Y. Carbon dot-based inorganic-organic nanosystem for two-photon imaging and biosensing of pH variation in living cells and tissues. Adv Mater. 2012; 24: 5844−8.
36. Zheng Y, Cheng Y, Chen J, Ding J, Li M, Li C, et al. Injectable Gel-MS construct with sequential degradation for locally synergistic chemotherapy. ACS Appl Mater Interfaces. 2017; 9: 3487−96.
37. Deng X, Zhou S, Li X, Zhao J, Yuan M. *In vitro* degradation and release profiles for poly-DL-lactide-poly(ethylene glycol) microspheres containing human serum albumin. J Controlled Release. 2001; 71: 165−73.
38. Templin JS, Wylie MC, Kim JD, Kurgansky KE, Gorski G, Kheir J, et al. Neosaxitoxin in rat sciatic block improved therapeutic index using combinations with bupivacaine, with and without epinephrine. Anesthesiology. 2015; 123: 886−98.
39. Rwei AY, Lee JJ, Zhan C, Liu Q, Ok MT, Shankarappa SA, et al. Repeatable and adjustable on-demand sciatic nerve block with phototriggerable liposomes. Proc Natl Acad Sci U S A. 2015; 112: 15719−24.
40. Zhan C, Wang W, McAlvin JB, Guo S, Timko BP, Santamaria C, et al. Phototriggered local anesthesia. Nano Lett. 2016; 16: 177−81.
41. Lu L, Zhang W, Wu X, Wang X, Zhang M, Zhu Q, et al. A novel ropivacaine-loaded *in situ* forming implant prolongs the effect of local analgesia in rats. Arch Med Sci. 2013; 9: 614−21.
42. Kouchi M, Shibayama Y, Ogawa D, Miyake K, Nishiyama A, Tamiya T. (Pro)renin receptor is crucial for glioma development via the Wnt/β-catenin signaling pathway. J Neurosurg. 2017: 1−10.
43. Tang J, Kong B, Wu H, Xu M, Wang Y, Wang Y, et al. Carbon nanodots featuring efficient FRET for real-time monitoring of drug delivery and two-photon imaging. Adv Mater. 2013; 25: 6569−74.
44. Nau C, Wang G. Interactions of local anesthetics with voltage-gated Na^+ channels. J Membrance Biol. 2004; 201: 1−8.
45. Bailard NS, Ortiz J, Flores RA. Additives to local anesthetics for peripheral nerve blocks: Evidence, limitations, and recommendations. Am J Health-Syst Pharm. 2014; 71: 373−85.
46. McDowell TS, Durieux ME. Chapter 33 - Pharmacology of local anesthetics A2 - Hemmings, Hugh C. In: Hopkins PM, editor. Foundations of Anesthesia (Second Edition). Edinburgh: Mosby. 2006: 393−401.
47. Cheung EY, Harris KD, Johnston RL, Kitchin SJ, Hadden KL, Zakrzewski M. Rationalizing the structural properties of bupivacaine base—A local anesthetic—directly from powder X-ray diffraction data. J Pharm Sci. 2004; 93: 667−74.
48. Hirota K, Kawamoto T, Nakajima T, Makino K, Terada H. Distribution and deposition of respirable PLGA microspheres in lung alveoli. Colloids Surf, B. 2013; 105: 92−7.
49. Liu X, Miller ALII, Yaszemski MJ, Lu L. Biodegradable and crosslinkable PPF-PLGA-PEG self-assembled nanoparticles dual-decorated with folic acid ligands and Rhodamine B fluorescent probes for targeted cancer imaging. RSC Adv. 2015; 5: 33275−82.
50. Gao Y, Ren F, Ding B, Sun N, Liu X, Ding X, et al. A thermo-sensitive PLGA-PEG-PLGA Gel for sustained release of docetaxel. J Drug Targeting. 2011; 19: 516−27.
51. Wang P, Zhuo X, Chu W, Tang X. Exenatide-loaded microsphere/thermosensitive Gel long-acting delivery system with high drug bioactivity. Int J Pharm. 2017; 528: 62−75.
52. Zhang XZ, Lewis PJ, Chu CC. Fabrication and characterization of a smart drug delivery system: Microsphere in Gel. Biomaterials. 2005; 26: 3299−309.
53. Chen SB, Pieper R, Webster DC, Singh J Triblock copolymers: Synthesis, characterization, and delivery of a model protein. Int J Pharm. 2005; 288: 207−18.
54. Belete MFA. Formulation of sustained release floating microspheres of furosemide from ethylcellulose and hydroxypropyl methylcellulose polymer blends. J Nanomed Nanotechnol. 2015; 06: 1000262.
55. McAlvin JB, Padera RF, Shankarappa SA, Reznor G, Kwon AH, Chiang HH, et al. Multivesicular liposomal bupivacaine at the sciatic nerve. Biomaterials. 2014; 35: 4557−64.
56. Epstein-Barash H, Shichor I, Kwon AH, Hall S, Lawlor MW, Langer R, et al. Prolonged duration local anesthesia with minimal toxicity. Proc Natl Acad Sci U S A. 2009; 106: 7125−30.
57. El-Boghdadly K, Chin KJ. Local anesthetic systemic toxicity: Continuing professional development. Can J Anaesth. 2016; 63: 330−49.
58. Tofoli GR, Cereda CMS, Araujo DR, Franz-Montan M, Groppo FC, Quaglio D, et al. Pharmacokinetic study of liposome-encapsulated and plain mepivacaine formulations injected intra-orally in volunteers. J Pharm Pharmacol. 2012; 64: 397−403.

59. Powers BL, Wing DA, Carr D, Ewert K, Di Spirito M. Pharmacokinetic profiles of controlled-release Gel polymer vaginal inserts containing misoprostol. J Clin Pharmacol. 2008; 48: 26−34.
60. Wang W, Tao H, Zhao Y, Sun X, Tang J, Selomulya C, et al. Implantable and biodegradable macroporous iron oxide frameworks for efficient regeneration and repair of infracted heart. Theranostics. 2017; 7: 1966−75.
61. Sun X, Kong B, Wang W, Chandran P, Selomulya C, Zhang H, et al. Mesoporous silica nanoparticles for glutathione-triggered long-range and stable release of hydrogen sulfide. J Mater Chem B. 2015; 3: 4451−7.
62. Kong B, Tang J, Zhang Y, Jiang T, Gong X, Peng C, et al. Incorporation of well-dispersed sub-5-nm graphitic pencil nanodots into ordered mesoporous frameworks. Nat Chem. 2016; 8: 171−8.
63. Paula E, Cereda CMS, Fraceto LF, de Araújo DR, Franz-Montan M, Tofoli GR, et al. Micro and nanosystems for delivering local anesthetics. Expert Opin Drug Delivery. 2012; 9: 1505−24.
64. Urbanski W, Marycz K, Krzak J, Pezowicz C, Dragan S. Cytokine induction of sol-gel-derived TiO_2 and SiO_2 coatings on metallic substrates after implantation to rat femur. Int J Nanomed. 2017; 12: 1639−45.
65. Lu J, Yuan XS, Guo ZQ, Xu R, Yi LH. Bupivacaine induces apoptosis via mitochondria and p38 MAPK dependent pathways. Eur J Pharmacol. 2011; 657: 51−8.